International Journal of Environmental Science and Technology (2026) 23:336
https://doi.org/10.1007/s13762-026-07095-3

ORIGINAL PAPER

Treatment of landfill leachate and production of geopolymer using electrocoagulation sludge

A. Aşkın[1] · H. K. Kırıkbıçak[1] · E. Arıöz[2] · Ü. Tezcan Ün[3]

Received: 26 November 2024 / Revised: 13 January 2026 / Accepted: 28 January 2026 / Published online: 7 March 2026
© The Author(s) 2026

Abstract

This study employed an innovative electrocoagulation method to treat landfill leachate, utilizing uniquely designed aluminum electrodes. The investigation focused on the effects of various parameters on treatment efficiency, including initial pH, current density, NaCl concentration, and stirring rate. Results demonstrated that the initial COD concentration of 9600 mg/L was reduced to 282 mg/L at a pH of 5, 40 mA/cm^2, 0.1 M NaCl concentration, and stirring rate of 60 rpm with the removal efficiency of 97%, meeting direct discharge limits. Additionally, successful removal of phosphorus and nitrogen was achieved, underscoring the comprehensive treatment capabilities of electrocoagulation. Furthermore, electrocoagulation sludge was repurposed for geopolymer production, highlighting the potential for sustainable waste management practices. These findings offer valuable insights for optimizing landfill leachate treatment strategies while promoting environmental sustainability and presenting an excellent opportunity for industrial symbiosis.

Highlights

- An innovative electrocoagulation method was employed for the treatment of landfill leachate, utilizing uniquely designed aluminum electrodes.
- Successful removal of COD, phosphorus, and nitrogen was a noteworthy achievement that meets the criteria for direct discharge into water bodies.
- Treatment efficiency was optimized by examining the effects of parameters such as initial pH, current density, NaCl concentration, and stirring rate.
- The utilization of electrocoagulation sludge as raw material for geopolymer production represents a sustainable approach to waste management and resource utilization.

Keywords Aluminum · Electrocoagulation · Geopolymer · Leachate · Wastewater

Introduction

Landfill wastewater or landfill leachate, is primarily generated by rainfall, surface runoff, and groundwater infiltration as it percolates through the landfill (Li et al. 2011). Landfill leachate presents a significant environmental challenge due to its highly complex and toxic composition resulting from the decomposition of organic waste materials. Numerous contaminants, including heavy metals, organic compounds, nitrogen, phosphorus, and microorganisms, are present in landfill leachate and pose a significant environment and public health risk (Li et al. 2017; Asaithambi et al. 2018). Effective landfill leachate treatment is imperative to prevent groundwater, surface water, and soil contamination and

Editorial responsibility: S.Mirkia

✉ A. Aşkın
aaskin@ogu.edu.tr

[1] Department of Chemical Engineering, Faculty of Engineering and Architecture, Eskişehir Osmangazi University, 26040 Eskisehir, Turkey

[2] Department of Chemical Engineering, Faculty of Engineering, Eskişehir Technical University, 26555 Eskisehir, Turkey

[3] Department of Environmental Engineering, Faculty of Engineering, Eskişehir Technical University, 26555 Eskisehir, Turkey

mitigate the associated environmental and public health risks (Mansour et al. 2021).

Landfill leachate can be treated using including biological, physical, or chemical techniques. Biological treatment methods, such as anaerobic and aerobic treatments, have certain limitations. Due to the organic carbon's resistant nature, they may not effectively treat old landfill leachate with limited biodegradability (Guo et al. 2022).

While physiochemical techniques such as advanced oxidation, ultrafiltration, dissolved air flotation, neutralization, membrane filtration, reverse osmosis, and coagulation-flocculation can be used to treat landfill leachate, they have limitations such as high operating costs, decreased efficiency in removing pollutants, and reduced process performance, which is why an effective and economical treatment process needs to be designed and developed (Faheem et al. 2021; Asaithambi et al. 2018).

Electrochemical technologies which have several advantages for wastewater treatment methods, including exceptional performance in eliminating persistent contaminants, adaptability, environmental friendliness, and possible cost-effectiveness (Martı´nez-Huitle et al., 2006). ElectroCoagulation (EC) has appeared as a promising and versatile method for treating of various types of wastewater, including landfill leachate (Ramprasad et al., 2019).

Several researchers performed electrochemical treatment of landfill leachate. The electrocoagulation/anodic oxidation was performed using iron and boron-doped diamond electrodes (Fernandes et al. 2015). The treatment of landfill leachate was also achieved by the Electro-Fenton (EF) method with a COD removal efficiency of 72% (Atmaca 2009). Anglada et al. (2011) investigated the efficacy of boron-doped diamond material for electrochemical leachate oxidation. Achieved 51% COD with a current intensity of 2571 Am^{-2} after 8 h of reaction time (Anglada et al. 2011). Ilhan et al. (2008) found that electrocoagulation using iron and aluminum electrodes reduced chemical oxygen demand (COD) by 56% and removed 24% of ammonia in 30 min at 631 A/m^2. Tezcan Un et al. (2018) treated the landfill leachate using integrated continuous electrocoagulation and the anaerobic treatment technique (Tezcan Un et al. 2018). Electrocoagulation of leachate was also achieved by monopolar aluminum electrodes, which provided 57% COD removal (Tezcan Un and Oduncu,, 2014).

During electrocoagulation, a direct current is applied to aluminum or iron electrodes that act as sacrificial anodes. As a result of this process, the electrodes are dissolved, and their cations are produced. The metal ions that are generated are then hydrolyzed in the electrochemical cell, leading to the formation of metal hydroxide ions, as shown in reactions (1)–(3) (Tezcan Un and Oduncu 2014; Bazrafshan et al. 2012).

$$Al \rightarrow Al^{+3}(aq) + 3e^{-} \quad (1)$$

$$Al^{+3}(aq) + 3H_2O \rightarrow Al(OH)_3(s) + 3H^{+}(aq) \quad (2)$$

$$nAl(OH)_3 \rightarrow Al_n(OH)_3n \quad (3)$$

Despite the high removal efficiency achieved through electrocoagulation (EC), the formation of sludge during the process can lead to waste management issues due to the high content of aluminum present in the sludge. It is worth noting that geopolymers utilize aluminum, which means that the sludge generated during the electrocoagulation process can be repurposed for geopolymer production.

Geopolymers, as an alternative to Portland cement, often offer several advantages in terms of cost and overall systemic environmental implications (Jamieson et al. 2015). Geopolymers, silico-aluminate materials created by simulating the natural rock-forming process, are quickly becoming a new class of building materials for green structures (Kumar et al. 2007). They are made by blending an alkaline activator containing alkali hydroxide, silicates, aluminates, carbonates, or sulfates with a reactive aluminosilicate powder (such as fly ash, metakaolin, or calcined clay) (Castillo, 2022). The chemical compositions of the source materials affect the microstructural development and mechanical properties of geopolymers (Nath and Sarker 2017). Industrial waste materials like fly ash and blast furnace slag can be used to produce geopolymer, besides natural sources such as kaolinite (Sudagar et al. 2023). Due to the high annual production, the presence of amorphous phases, the sphere geometry of low-size particles, and the relatively stable chemical composition, geopolymers are more commonly produced using Class F fly ash (Freire, 2020; Xu et al. 2021).

Geopolymers have gained increasing attention in recent years for their applications in various sectors, including construction, wastewater treatment, and environmental remediation (Sudagar et al. 2023). They offer advantages such as low cost, high strength, durability, and environmental friendliness, making them an attractive alternative to traditional materials and treatment methods.

This study aims to investigate the efficacy of electrocoagulation for treating landfill leachate, utilizing a unique electrode design comprising a cylindrical aluminum vessel serving as the cathode and a mechanical mixer with four aluminum blades acting as the anode. By examining the effects of parameters such as initial pH, current density, NaCl concentration, and stirring rate, this study aims to optimize treatment efficiency and highlight the potential for utilizing electrocoagulation sludge as repurposed for geopolymer production. This study's unique design and approach distinguish it from existing literature, offering

Table 1 Characteristics of landfill leachate

Parameter	Value	Limit value*
pH	7.97	6.00–9.00
COD (mg/L)	9600	700
Phosphorus (mg/L)	2.72	2.00
Nitrogen (mg/L)	49	20

*Water Pollution Control Regulations of Turkey (2004) (Table 20.6)

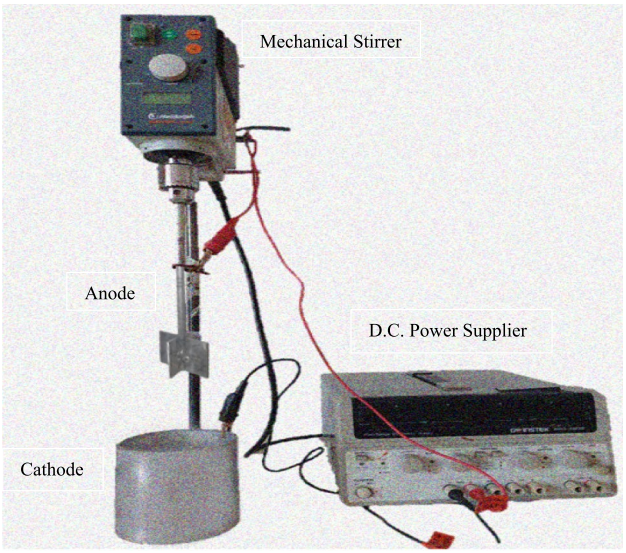


Fig. 1 Experimental setup

valuable insights for developing sustainable and effective landfill leachate treatment strategies. Afterward, to lessen the sludge's environmental impacts, the sludge created during the electrocoagulation of landfill leachate was used to produce geopolymer. This novel application of electrochemical sludge, is typically considered a waste product in electrocoagulation processes and presents an excellent opportunity for industrial symbiosis.

Material and methods

Electrochemical treatment of leachate

Wastewater

The experiments used landfill leachate obtained from the Kutahya Solid Waste Sanitary Landfill area in Turkey. Table 1 shows the characteristics of landfill leachate and the limiting value according to the Water Pollution Control Regulation of Turkey (2004).

Experimental setup

The electrocoagulation experiments were performed at the aluminum reactor. The cathode was a cylindrical aluminum reactor with dimensions of 10 cm in diameter and 10 cm in height. The anode was an aluminum stirrer with four rectangular blades (3 cm × 2.35 cm). The total available anode area (blade area) was 564 cm^2. It was placed in the reactor's center. The experimental setup is presented in Fig. 1.

500 ml of leachate was added to the cathode vessel for each run. Every run was done at room temperature. The pH values were adjusted to the desired value using either H_2SO_4 or NaOH solutions. The anode blades are located in the center of the cathode vessel and submerged in the wastewater. The sample was agitated at 80 rpm using anode blades connected to the mechanical stirrer (Heidolph RZR 2102). The anode and cathode were connected to the DC power source (GW Instek SPD-3606) using copper wire. During electrocoagulation, the pH and conductivity were measured with a pH meter (Hanna Ins. 301) and a conductivity meter (Radiometer Pioneer 30). The experiments were performed at 120 min. After conducting electrocoagulation of wastewater using aluminum electrodes, the resulting sludge was collected and dried. The dried sludge was then utilized in the production of geopolymer.

Analyses

Samples were taken periodically centrifuged, and the supernatant was analyzed to determine Chemical Oxygen Demand (COD) concentration using the Closed Reflux Titrimetric Method based on the American Society for Testing and Materials, 1995 (American Society for Testing and Materials, 1995). All analyses were done twice, and the average was used. The phosphorus and nitrogen concentrations were determined at Hach Lange Dr 2800 Spectrophotometer using the relevant kits (LCK 349 and LCK 138, respectively).

The following equation was used to obtain the removal efficiency (RE%).

$$RE\% = \frac{C_0 - C}{C_0} \times 100 \quad (4)$$

where C_0 and C represent the concentrations in milligrams per liter before and after the treatment, respectively.

The electrical energy consumption was calculated as kW h per m^3 of treated effluent, as seen from Eq. (5) (Pletcher and Walsh 2012).

$$EC = \frac{VIt}{v} \quad (5)$$

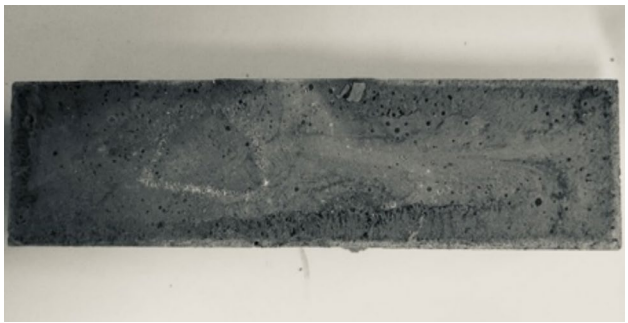


Fig. 2 Photograph of geopolymer after aging process

where EC is the electrical energy consumption (kW h/m^3), V is the potential (Volt), I is the current (Amper), t is the time (hour), and v is the volume of the solution treated (m^3).

Geopolymer production and characterization

In the geopolymerization process, condensation reactions are initiated by aluminum. Therefore, it is desirable to initially have a high aluminum content (Peng et al. 2015). For this reason, the goal is to evaluate the aluminum-containing electrocoagulation sludge obtained from the electrochemical treatment of leachate as substituent material for geopolymer production highlights in the geopolymerization process. Geopolymerization was achieved using class F fly ash from the Thermal Power Plant in Zonguldak, Turkey. 14 M NaOH was used as an alkaline solution in the synthesis. The alkaline solution was added to solid raw material at a ratio of 0.5. Waste material resulting from the electrocoagulation process was added to fly ash in varying ratios of 1%, 3%, and 5% by weight. Geopolymer pastes were mixed for 10 min to get a homogeneous paste and then cured at 100 °C for 24 h. After curing, pastes were aged for 28 days at laboratory conditions and grounded for characterization. The appearance of the geopolymer produced from electrocoagulation sludge after the aging process is shown in Fig. 2.

Crystalline phases of samples were determined by X-ray diffractometer (XRD) (Panalytical EMPYREAN, Germany) with CuKα radiation operated at 45 kV and 35 mA in the range of 10–80°2θ. Fourier transform infrared spectroscopy (FTIR) (PerkinElmer Spectrum Two, USA) between 400 and 4000 cm^{-1} with a resolution of 4 cm^{-1} was used to analyze the functional groups using the KBr method. X-ray fluorescence (XRF) (Rigaku, ZSX, Germany) analyses were performed using the solid sample method. Nuclear magnetic resonance spectroscopy (NMR) (JEOL ECZ500R, 11.75 Tesla) analyses were carried out using NMR 27 Al and Si method. HNO_3, H_2O_2, and HF acids were used inductively coupled plasma mass spectrometry (ICP-MS) (Thermo iCAP RQ) analysis as reagents. The surface morphological structure of geopolymers was observed by Scanning Electron Microscope (SEM) (JEOL JSM-5600LV).

All the above-mentioned characterization analyses of the geopolymer samples were carried out at Eskişehir Osmangazi University Central Research Laboratory Application and Research Center.

Results and discussion

Electrocoagulation of landfill leachate

This study optimized electrocoagulation parameters through experimental evaluation, focusing on COD removal efficiency, energy consumption, and achieving a dischargeable effluent quality. Instead of applying mathematical optimization models, the best operating conditions were determined by systematically adjusting key parameters and assessing their impact on treatment performance. This practical, results-driven approach highlights the effectiveness and sustainability of electrocoagulation as a viable treatment method for landfill leachate.

The effect of the initial pH

The pH level of the solution undergoing electrocoagulation is a critical factor, as it directly affects the generation of hydroxide ions (OH^-). At the cathode, water reduction occurs, leading to the producing hydroxide ions (OH^-) and hydrogen gas. These OH^- ions play a key role in contaminants' coagulation and subsequent precipitation.

Understanding the pH-dependent mechanisms at work during electrocoagulation is essential to optimizing the process for efficient COD removal. The impact of the initial pH on the COD removal was determined at 40 mA/cm^2 using initial pH values of 3, 5, 7, and 9.

During the electrocoagulation process, the solution's pH increased, as seen in Fig. 3. The production of OH^- at the cathode contributed to the increase in pH. The OH^- generated at the cathode and Al^{3+} formed at the anode interact in the solution to form aluminum hydroxide, $Al(OH)_3$.

Figure 4 shows the COD removal efficiencies at different initial pH. As seen from the figure, the highest COD removal efficiency of 85% was obtained at a pH of 5. The initial COD concentration of 9600 mg/L was reduced to the 1440 mg/L. Similarly, Bayar et al. found the initial pH of 5.2 more effective than the pH of 3 for removing of COD from wastewater (Bayar et al. 2015).

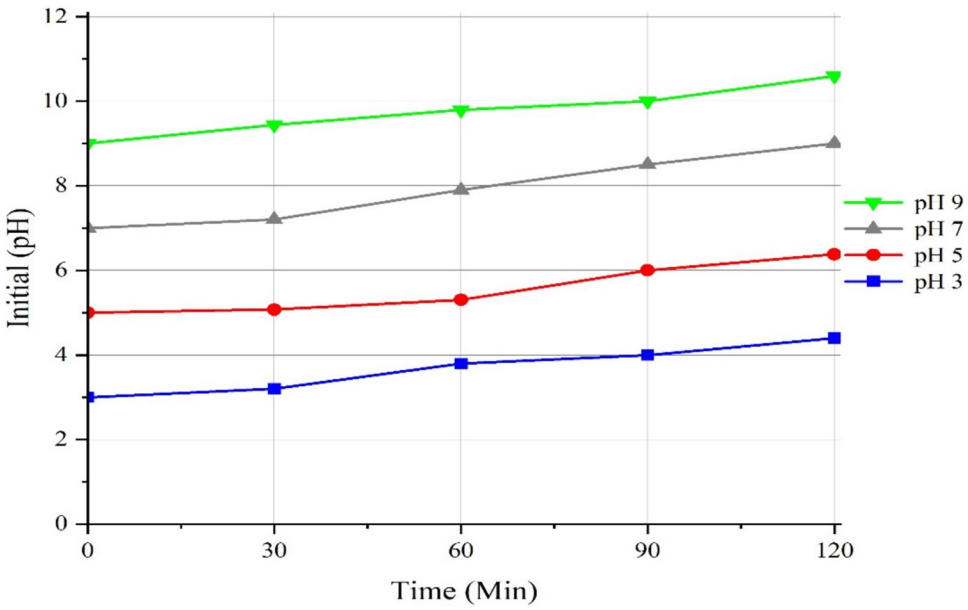


Fig. 3 The change of initial pH with time during electrocoagulation

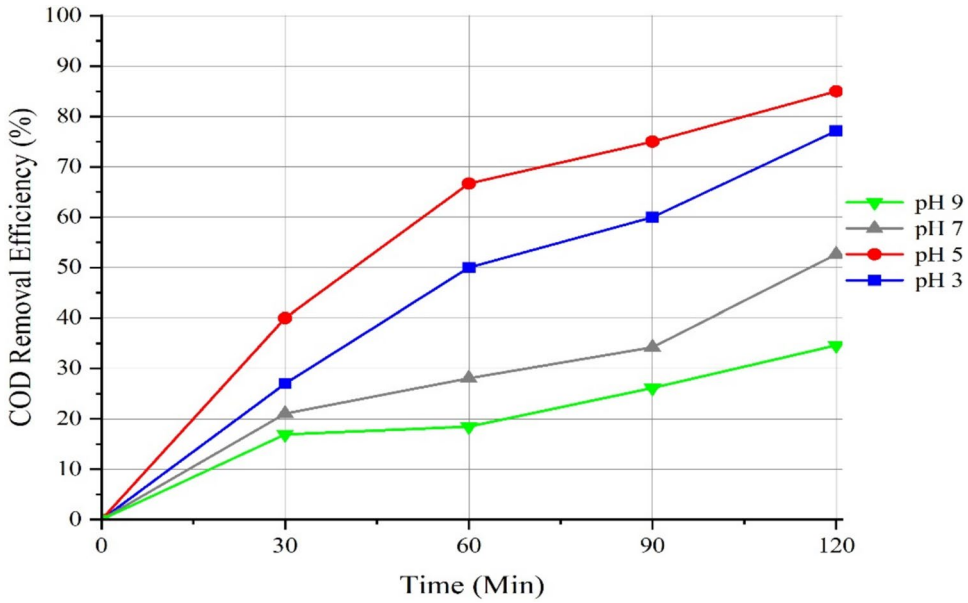


Fig. 4 The effect of the initial pH on the COD removal efficiency, i: 40 mA/cm^2

This finding can be attributed to forming aluminum hydroxide precipitates, which effectively adsorb and coagulate COD. As seen in Fig. 4, the removal efficiencies were reduced in the more acidic or basic environments. Lower pH values promote H_2 gas evolution, which competes with COD removal, ultimately decreasing the overall treatment efficiency. Additionally, at lower pH values, the concentration of hydroxide ions decreases, which can lead to the dissolution of aluminum hydroxide, making it less effective as a coagulant. Conversely, at higher pH values, the excessive concentration of hydroxide ions can lead to the formation of soluble aluminum complexes, which may also reduce the effectiveness of aluminum hydroxide as a coagulant.

The effect of the current density

The most important operating parameter is the current density, which affects how much aluminum is produced, is. Various studies have been conducted to determine the effect of current density, specifically at values of 30, 40, 50, and 60 mA/cm^2 at pH 5.

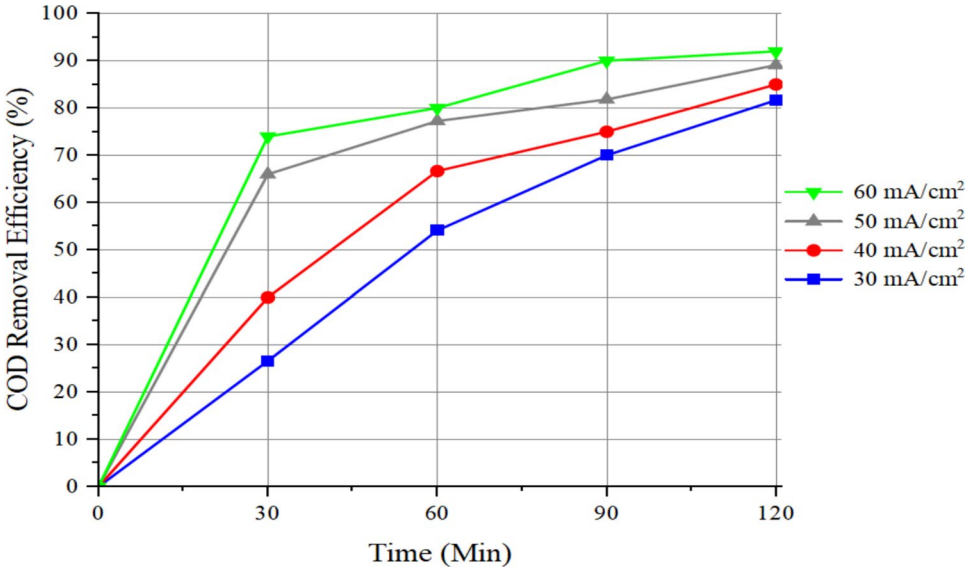


Fig. 5 The effect of the current density on the COD removal efficiency, pH: 5, 80 rpm

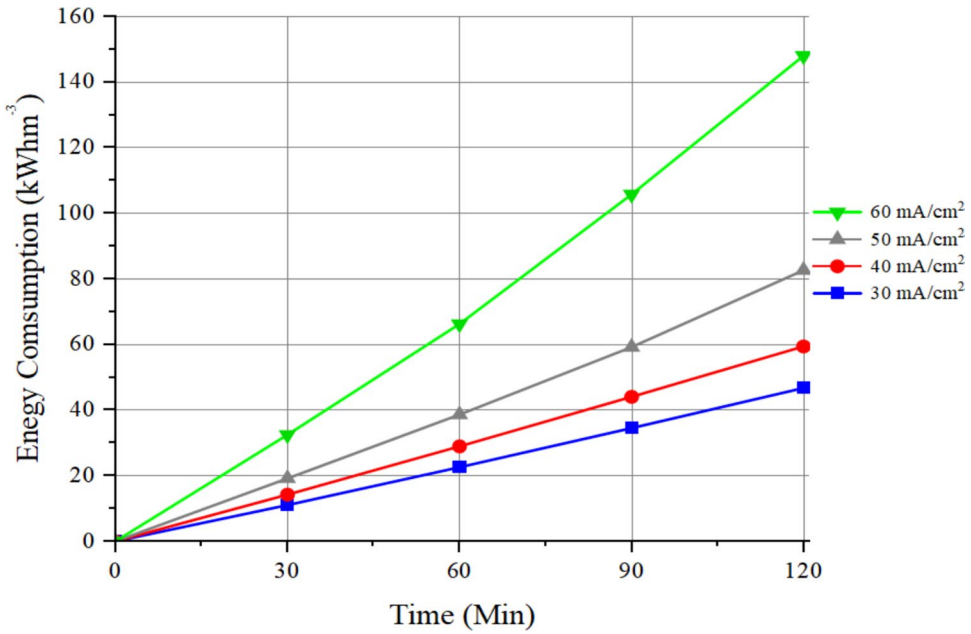


Fig. 6 The energy consumptions for different current densities, pH: 5, 80 rpm

The experimental results, as seen in Fig. 5, indicated that as the current density increased from 30 to 60 mA/cm^2, the removal efficiency of COD also increased from 82 to 92%. The initial COD concentration of 9600 mg/L was reduced to 768 mg/L at 60 mA/cm^2. The higher current densities result in a greater quantity of aluminum ions (Al^{3+}) being generated at the anode due to the oxidation of aluminum as per Faraday's Law (Eq. 6), which states that the amount of substance (metal ions) dissolved during the electrochemical reaction is directly proportional to the quantity of electricity passing through the system (Brett and Brett 1993). This increased generation of aluminum ions contributes to forming $Al(OH)_3$ coagulant precipitates, which aid in removing contaminants from the wastewater. A similar result was obtained by Galvão et al. for the treatment of landfill leachate (Galvão et al. 2020).

$$m = \frac{itM}{nF} \tag{6}$$

where M is the molecular weight of Al (M = 27), n is the number of electrons that participate in the oxidation reaction (n = 3), i the current density (A/cm^2), F is Faraday's constant (96,500 C/mol), t is the time (s), and m is the amount of dissolved aluminum (g Al/cm^2).

Current density is directly proportional to the electrical energy consumption of the electrocoagulation system. This means that as the current density increases, the energy

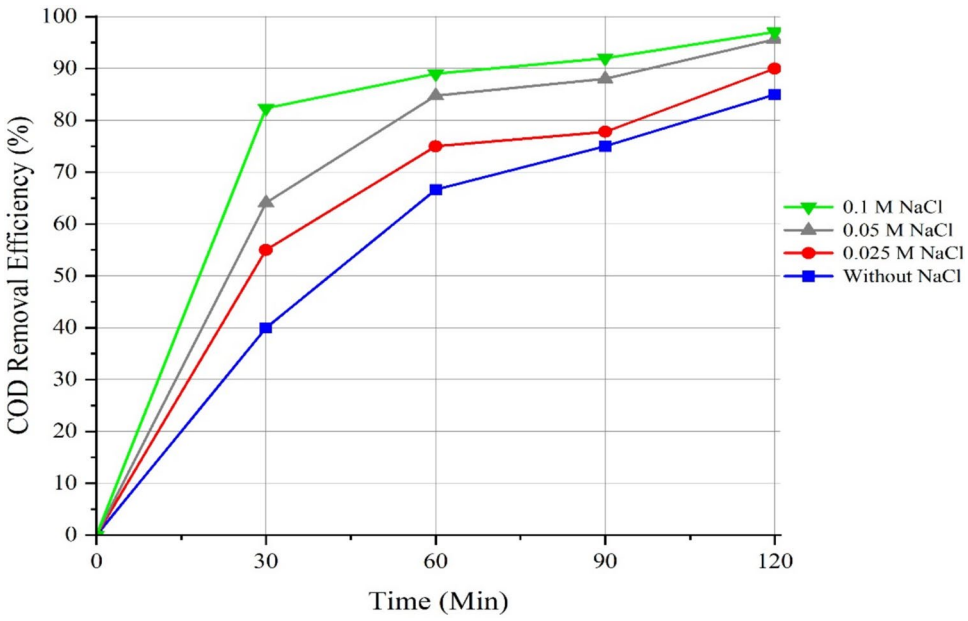


Fig. 7 The effect of the supporting electrolyte concentration on the COD removal efficiency, i: 40 mA/cm^2, pH: 5, 80 rpm

consumed by the process also increases. The energy consumptions were 46.7, 59.4, 82.6, and 148.0 kW h/m^3 for 30, 40, 50, and 60 mA/cm^2 at the end of 120 min, respectively, as seen in Fig. 6. Therefore, balancing the desired removal efficiency with energy consumption is crucial for optimizing electrocoagulation processes. Evaluate whether the improved removal efficiency justifies the increase in energy usage regarding sustainability and carbon footprint. Because of the energy consumption, subsequent experimental studies were carried out at 40 mA/cm^2.

The effect of the supporting electrolyte concentration

Electrocoagulation relies on the flow of electric current through the wastewater to drive the electrochemical reactions at the electrodes. One primary role of the supporting electrolyte, NaCl, is to increase the electrical conductivity of the solution. Higher conductivity reduces the electrical resistance within the system, ensuring a more efficient transfer of electrons and ions during the process. The effect of NaCl concentration on the COD removal efficiency was

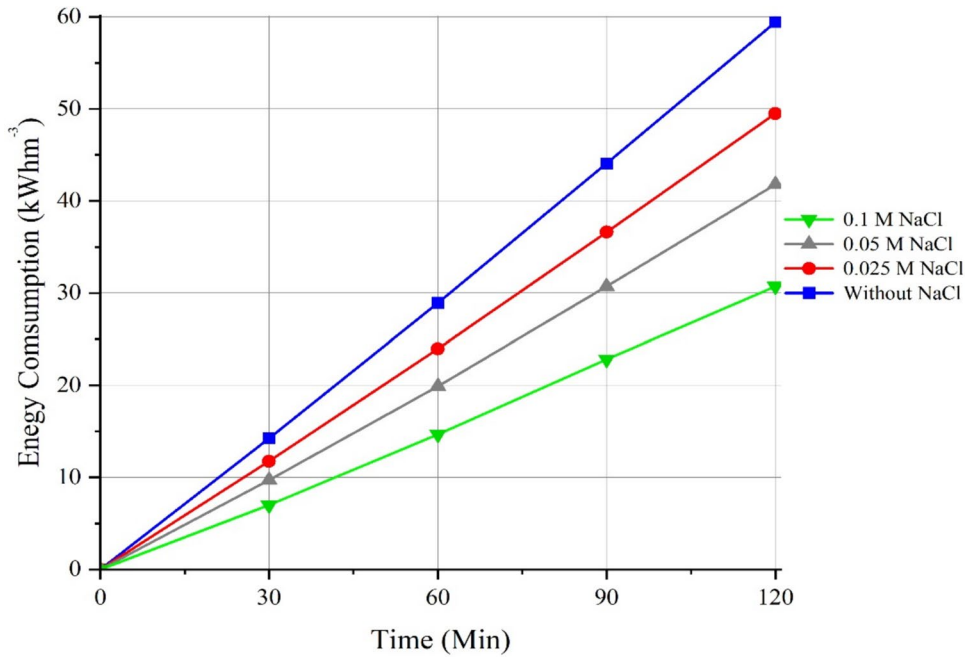


Fig. 8 The energy consumption for different supporting electrolyte concentrations, i: 40 mA/cm^2, pH: 5, 80 rpm

investigated using 0.1 M, 0.05 M, and 0.025 M NaCl concentrations at 40 mA/cm^2 and pH 5. The experiment was also performed without using NaCl; the results can be seen in Fig. 7.

As seen from Fig. 7, as the NaCl concentration increases, so does the removal efficiency of COD. The removal efficiency of 85% obtained without NaCl was increased to 97.0% with 0.1 M NaCl. The significant reduction of the initial COD concentration from 9600 to 282 mg/L with the use of 0.1 M NaCl as the supporting electrolyte indicates the remarkable success of the electrocoagulation process in wastewater treatment.

This low COD value signifies that the treated effluent meets the criteria for being directly dischargeable into the water bodies, underscoring the effectiveness and environmental significance of the electrocoagulation process. Additionally, the higher concentration of Cl^- ions generated at the anode accelerates the breakdown of organic contaminants, contributing to the higher removal efficiency. Increasing the NaCl concentration improved both chemical oxidation and electrocoagulation. Similarly, Li et al. demonstrated that raising the Cl concentration from 819 to 2500 mg/L increased the COD removal effectiveness from 29.8 to 38.9% (Li et al. 2011).

Higher NaCl concentrations significantly enhance the solution's electrical conductivity, reducing resistance. This promotes more effective electrocagulation with increased contact between organic materials and coagulants. As seen in Fig. 8, the electrical energy consumption of 59.4 kW h/m^3 was reduced to 30.7 kW h/m^3 with the use of 0.1 NaCl.

The effect of the stirring rate

The stirring rate within the reactor is one of the critical operational parameters that can significantly influence the transportation of dissolved ions from the electrode surface to the bulk solution. The effect of stirring rate on the removal of COD was evaluated using stirring rates of 60, 80, and 100 rpm in the presence of 0.1 M NaCl at pH 5 and 40 mA/cm^2.

As seen in Fig. 9, the removal efficiency was reduced from 97 to 90% with the increasing stirring rate from 60 to 100 rpm. Lower stirring rates allow for gentler agitation, which can lead to the formation of larger and more stable flocs. Larger flocs have a higher capacity to capture and entrap COD, resulting in more efficient removal (Liu et al. 2017). On the other hand, a higher stirring rate can create higher shear forces within the solution, potentially breaking apart or disintegrating the flocs prematurely, reducing their effectiveness in capturing COD. Lessoued et al. 2021 used aluminum electrodes to treat leachate in the electrocoagulation (EC) process to treat leachate. The process was conducted at mixing speeds ranging from 100 to 200 rpm, with the most favorable outcome being achieved at 150 rpm, resulting in a 90% removal of COD (Lessoued et al. 2021).

The phosphorus and nitrogen removal

Treating phosphorus and nitrogen in landfill leachate is of utmost importance before discharge due to the potentially harmful environmental impacts. The regulatory agencies

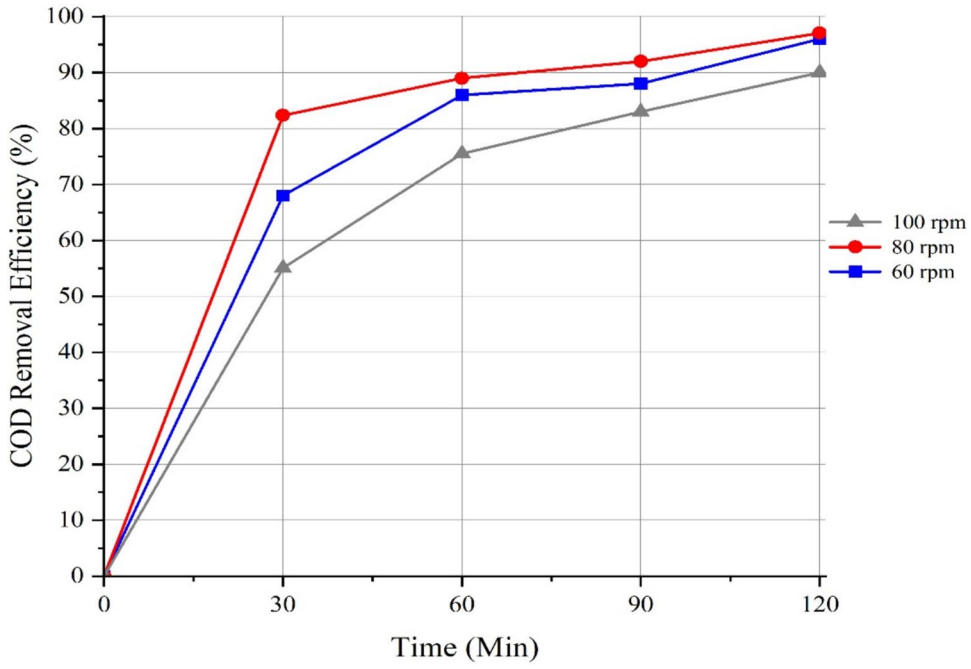


Fig. 9 The effect of the stirring speed on the COD removal efficiency, i: 40 mA/cm^2, pH: 5, 0.1 M NaCl

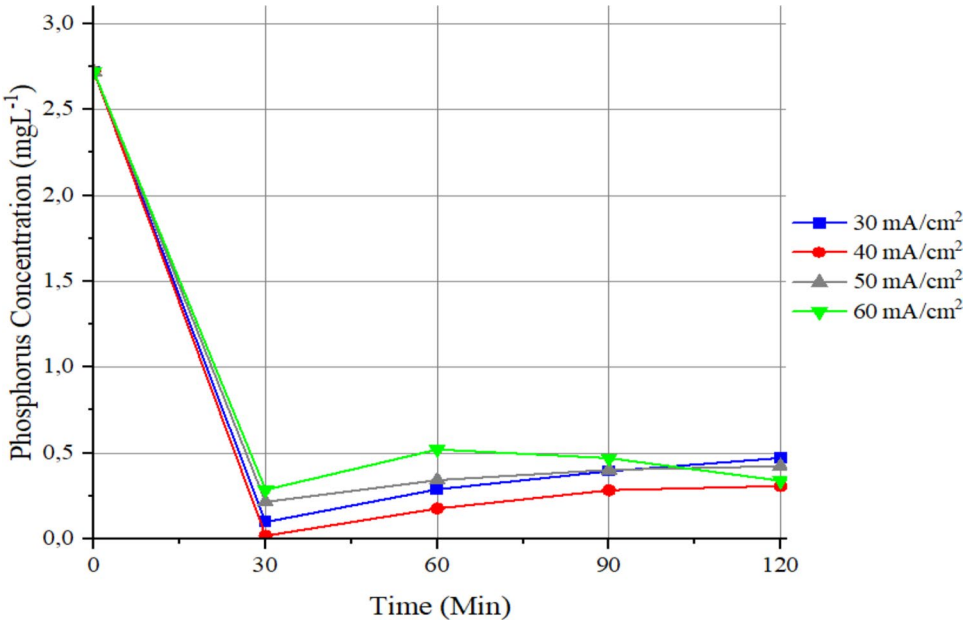


Fig. 10 The effect of the current density on the phosphorus concentration, pH: 5, 80 rpm, without NaCl

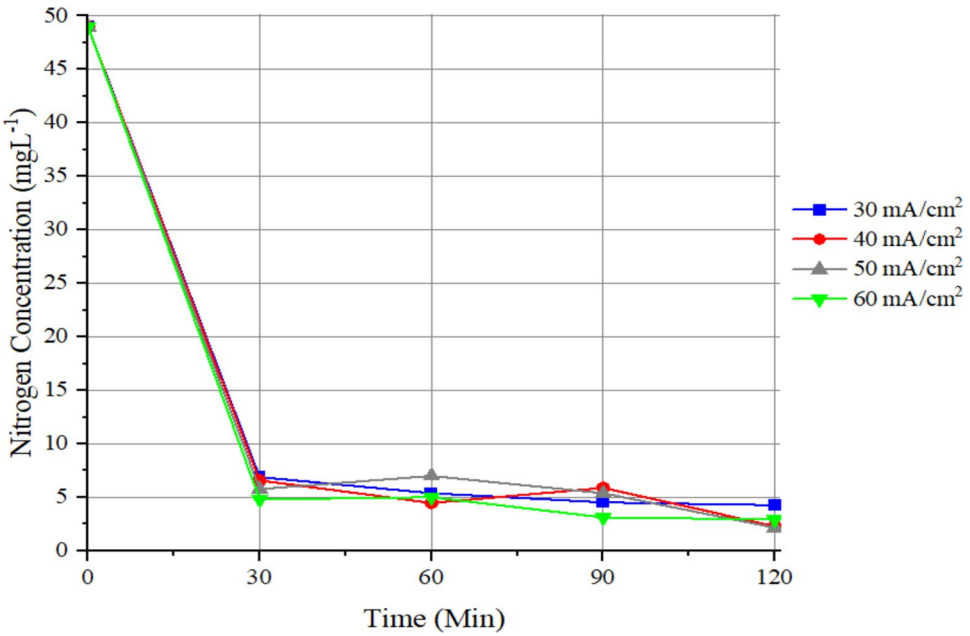


Fig. 11 The effect of the current density on the nitrogen concentration, pH: 5, 80 rpm, without NaCl

impose strict discharge limits to prevent eutrophication in receiving waters and safeguard both surface water quality and groundwater resources. Phosphorus and nitrogen removal was performed at pH 5 using different current densities. As seen from Figs. 10 and 11, at the first 30 min, the phosphorus concentration decreased from 2.72 to less than 0.5 mg/L at all current densities. The nitrogen concentration of 49 mg/L decreased to 5 mg/L after 30 min of electrocoagulation. These final concentrations not only meet but also fall significantly below the stringent environmental regulations in Turkey, ensuring the safe and compliant discharge of treated landfill leachate into the environment. This achievement underscores the effectiveness of the treatment process in mitigating potential environmental risks associated with these contaminants.

Performance comparison with literature

Comparative analysis in Table 2 reveals that many recent studies achieve high removal efficiencies mostly at lower initial pollutant loads or by employing complex multi-stage

Table 2 Comprehensive comparison of the present study with recent literature on landfill leachate treatment

Reference	Wastewater type	Treatment method	Electrode configuration	Initial COD (mg/L)	Optimal conditions	Removal efficiency (COD)	Energy/cost	Key novelty/difference
This work	Landfill leachate (Turkey)	Electrocoagulation (EC) + geopolymerization	Al (Mixer blade anode)/Al (cylindrical cathode)	9,600	pH 5 40 mA/cm^2 120 min	97%	30.7 kW h/m^3	Innovative mixer electrode design & sludge valorization for geopolymer
Zhang et al. (2026)	Industrial leachate	Hybrid peroxicoagulation-ozonation (PCO)	Al–Fe (Dual anode)	1,031	0.8 mA/cm^2 O_3 1.8 mg/min	62%	0.044 kW h/g TOC	Dual-anode system targeting refractory organics
Kundu & Kalamdhad (2026)	Young high-strength leachate	Sequential EC + packed bed upflow anaerobic filter (PBUAF)	Al–Al	72,321	152 A/m^2 10 min (EC)	93.9% Combined	N/A	Coupling EC as pretreatment for biological anaerobic filter to treat extremely high loads
Abu-Nassar et al. (2026)	Landfill leachate	Hybrid electrocoagulation—ultrasonic (EC-US)	Al–Al	2,145	10 V 25 min	95.1%	N/A	Investigating anode weight loss and ultrasonic synergy
Zahnoune et al. (2025)	Fresh leachate	EC in external-loop airlift reactor (ELAR)	Al (Plate)	6,730	pH 7.8 54 mA/cm^2 60 min	85%	12.3 kW h/m^3	Kinetic modeling using VOK-LF model; Airlift reactor design
Asaithambi et al. (2025)	Landfill leachate	Airlift—sono—electrocoagulation (AL/US/EC)	Fe–Fe	3,200	pH 7 1 A/dm^2 180 min	100%	6.5 kW h/m^3	Triple hybrid system combining ultrasound, airlift, and EC
Justen et al. (2025)	Concentrated leachate (NF/RO)	Sequential EC followed by electrooxidation (EO)	Fe (EC) + BDD/Al (EO)	2,420	14 A (EC) + 1 A (EO)	30% Integrated	High energy demand	Focus on toxicity reduction (Artemia salina) and removing emerging contaminants
Kumar et al. (2025)	Hazardous waste leachate	EC (Optimized via RSM)	Al–SS (Hybrid)	26,236	pH 5.9 11.5 mA/cm^2 101 min	87.3%	0.83 US $/m^3	Optimization of hybrid electrodes for high COD loads
Kundu et al. (2024)	Young landfill leachate	EC (Adsorption-assisted)	Al–Al	70,634	pH 7.35 15.3 mA/cm^2 57 min	83.6%	2.78 g Al/L (Electrode loss)	Kinetic analysis of EC treating extremely high-strength leachate
Ogedey & Oguz (2024)	Stabilized leachate	EC + Coal-based powdered activated carbon (CBPAC)	Al–SS	1,044	pH 5 25 mA/cm^2 40 min	92%	1.84 US $/kg COD	Single-reactor integrated EC with powdered activated carbon

Table 2 (continued)

Reference	Wastewater type	Treatment method	Electrode configuration	Initial COD (mg/L)	Optimal conditions	Removal efficiency (COD)	Energy/cost	Key novelty/difference
Núñez et al. (2024)	Biologically treated leachate	EC for irrigation reuse	Al–Mg Alloys	648	pH 5 15 mA/cm^2 15 min	52.9%	0.42 kW h/m^3	Focus on Sodium Absorption Ratio (SAR) reduction for agricultural reuse
Pinedo-Hernández et al. (2024)	Raw leachate	Pilot-scale EC + treatment wetland (TW)	Al–Fe	5,142	20 V 2 cm gap	91.5% Combined	N/A	Hybrid system combining EC with nature-based solutions (Canna indica wetland)
Akbar et al. (2024)	Landfill leachate	Integrated EC + zeolite adsorption	Al (Cylindrical)	N/A (NH_3 focus)	pH 5 14 mA/cm^2 75 min	50% NH_3 removal focus	N/A	Specific focus on Ammonia and Color removal using Zeolite
Karagozoglu (2023)	High-strength leachate	EC versus electro-fenton (EF)	Fe (Monopolar)	2,200	pH 7 150 A/m^2 30 min	37.9% (EC) vs. 71.7% (EF)	2.26 €/m^3 (EC)	Comparative cost/efficiency analysis of EC versus Electro-Fenton
Jegadeesan et al. (2023)	Landfill leachate	EC + solar photo fenton (SPF)	Fe–Al	5,120	pH 7 4 V 60 min	75% (EC only)	4.60 US $/$m^3$	Integration with solar energy for sustainability
Gautam et al. (2022)	Hazardous waste leachate	EC (Optimized via RSM)	Galvanized iron (GI)	~ 35,000	pH 750 mA/cm^2 240 min	89.7%	N/A	Use of Galvanized Iron electrodes and RSM optimization

Table 3 XRF analysis results (%)

Element	Reference	1%	3%	5%
Si	30.387	28.337	27.557	28.002
Al	13.115	12.789	12.752	13.289
Mg	1.115	1.026	1.012	1.027
Na	6.636	7.318	6.901	7.284
Fe	6.666	6.400	6.374	6.466
K	4.563	4.328	4.405	4.371
Ca	1.254	1.184	1.226	1.153
Ti	1.017	0.984	1.226	0.935

hybrid systems e.g., (Ogedey & Oguz 2024; Pinedo-Hernández et al. 2024). In contrast, this study demonstrates that optimizing the electrode configuration via a mechanical mixer anode allows for the treatment of high-strength leachate (9600 mg/L COD) with 97% efficiency in a single stage. This performance surpasses recently reported efficiencies for similar loads, such as the 87.3% removal reported by Kumar et al. (2025), proving the efficacy of the proposed reactor design. Overall, the comparison demonstrates that the proposed electrocoagulation system provides competitive or superior treatment performance while maintaining operational simplicity.

Geopolymer characterization

XRF analysis

Elemental level contents of geopolymer samples were determined by X-ray fluorescence Spectrometer (Panalytical Zetium) and given in Table 3. The XRF analysis results showed that the elemental values did not change meaningfully. Despite the addition of waste containing Al to the samples, it was observed that the Al content did not change significantly.

XRD analysis

XRD analysis indicated that all the samples have an amorphous structure with a broad hump between 16° and 40°θ which is an indicator of an amorphous silicon-aluminum gel phase (Fig. 12) (Xu et al. 2021; Aouan et al. 2023b). It was observed that no new crystal phase was formed in the structures of the samples, and all samples were composed of quartz and mullite. As the percentage of the waste increased to 5%, the intensity of mullite peaks increased, whereas the intensity of quartz peaks decreased. However, the height of the hump slightly decreased with increasing waste sludge.

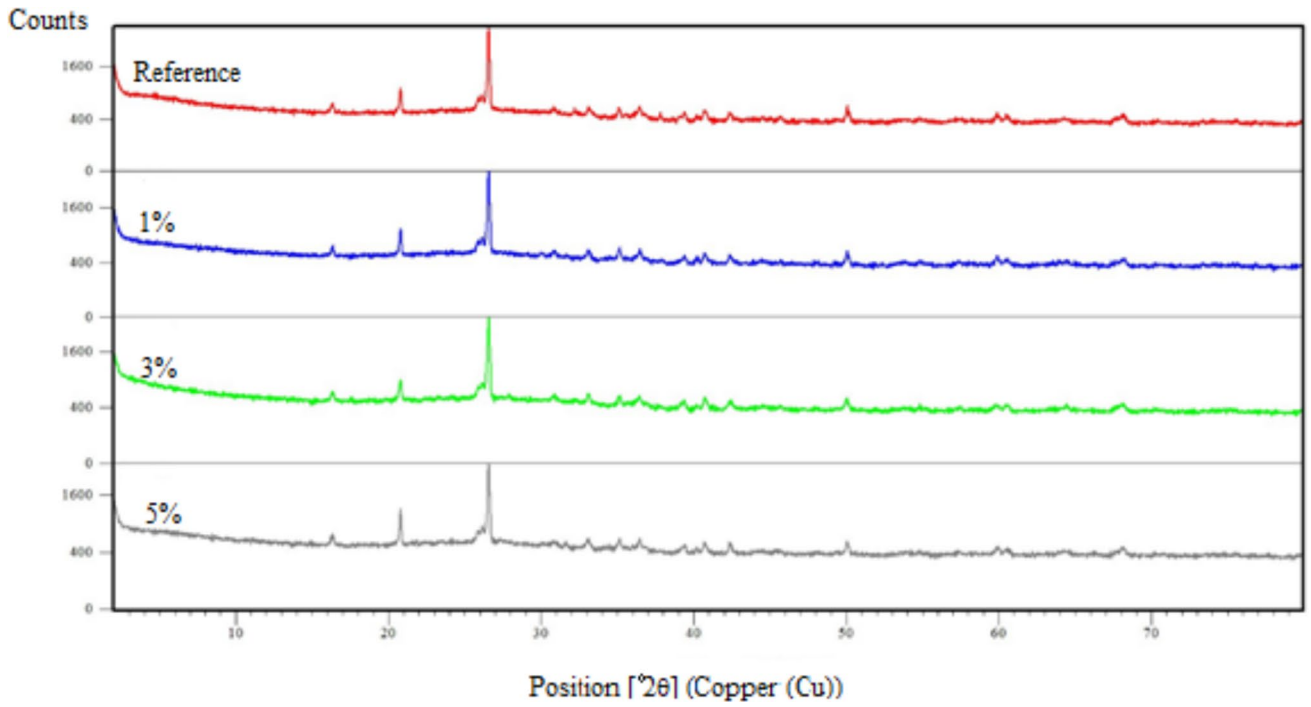


Fig. 12 XRD analysis charts for all samples

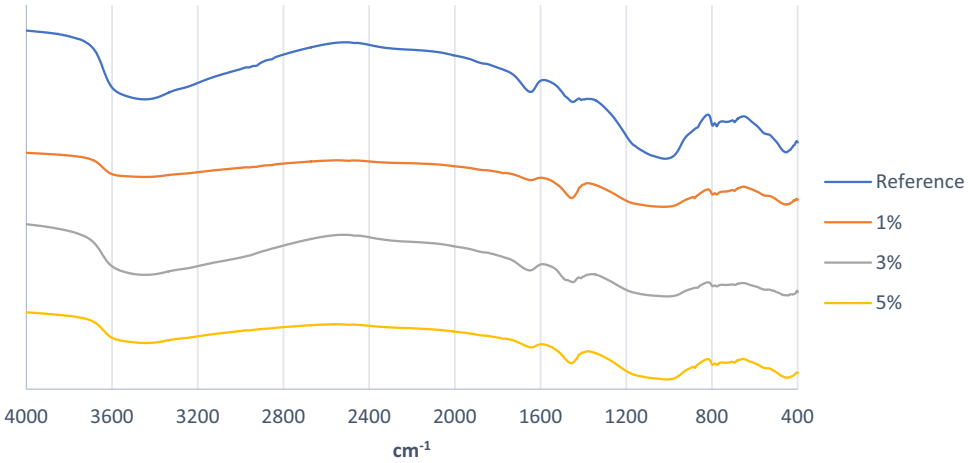


Fig.13 FTIR analysis charts for all samples

In general, an increase in the waste ratio was observed in mullite percentage values. The mullite ratio, which was 57.2% in the reference sample, increased to 59.2% with the addition of waste material. The peak intensity of the aluminum-containing mullite crystal was expected to increase due to the aluminum content of the waste added to the geopolymer samples.

FTIR analysis

The peaks observed between 1200 and 800 cm^{-1} are related to Si–O-T linkage asymmetric stretching vibrations (T = Si or Al) (Fig. 13) (Kuswah et al. 2021). The most substantial peak observed between these wavelengths indicates the fingerprint region of geopolymers (Ye et al. 2014; Jamil et al. 2020). The ring systems in geopolymers appear between 500 cm^{-1} and 800 cm^{-1} (Lecomte et al. 2006).

The prominent broad peaks observed at 1000 cm^{-1} are assigned to the asymmetrical stretching vibration of T–O (T=Al, Si), while T–O bending vibrations appeared at 450 cm^{-1} observed in all samples (Fernández-Jiménez and Palomo 2005; Criado et al. 2012; Yong-Sing et al. 2023). The peaks observed at 450 cm^{-1} are ascribed to in-plane Si–O bending vibrations in SiO_4 tetrahedra (Lecomte et al. 2006). The peaks observed approximately at 550 cm^{-1} are attributed to the octahedral aluminum in mullite existing in fly ash (Fernández-Jiménez and Palomo 2005; Kuswah et al. 2021). Two weak peaks indicating the presence of SiO_2 in the glassy phases were observed at 694 cm^{-1} and 777 cm^{-1}. The indistinct peaks observed at 797 cm^{-1} are attributed to O–Si–O regarding zeolites or geopolymers (Xu et al. 2021).

The bands at 1480 cm^{-1} and 870 cm^{-1} in all specimens are related to the out-of-plane bending of CO_3^{2-} (Xu et al. 2021; Liu et al. 2023). The broad peaks observed between and 3600 cm^{-1} are assigned to the O–H bond, and peaks seen approximately at 1650 cm^{-1} are attributed to H–O–H in the free water adsorbed on the surface or captured between the pores of the geopolymer samples (Aouan et al. 2023a).

It was observed that the peak was sharper in the reference sample and became more expansive as the amount of waste increased. This may indicate that side reactions occur due to the amorphous structure of the gel, indicating the replacement of Si^{4+} by Al^{3+} (Temuujin et al. 1999). The percentage of Al that can bind with Si increased with the amount of waste, but the shift to lower wavelengths can not be evaluated. While it was expected that the wavelength of the battery would shift to lower values as aluminum was added to the structure, this situation could not be observed (Poggetto et al. 2023).

SEM analysis

In the SEM image of the reference sample, it was seen that the texture of the sample was grainy (Fig. 14). The needle-shaped crystals were observed on the surface of the unreacted fly ash particle in the image of the sample prepared with 1% waste. Quartz and mullite crystal phases were not clearly observed in the structures of the samples. This may be due to the structure being amorphous and having a low degree of crystallinity (Huang and Wang 2021). It was also observed that more geopolymeric gel phases in a thin layer covered the surface of the unreacted fly ash particle.

ICP-MS analysis

ICP-MS analysis also shows the increase in Al the geopolymer structure with the increase in the waste ratio, as in the XRD diffractogram (Table 4). The release of Al values did not exceed the standards determined by the World Health Organization (WHO) (World Health Organization 2003). ICP analysis results show that aluminum waste is encapsulated inside the geopolymer structure.

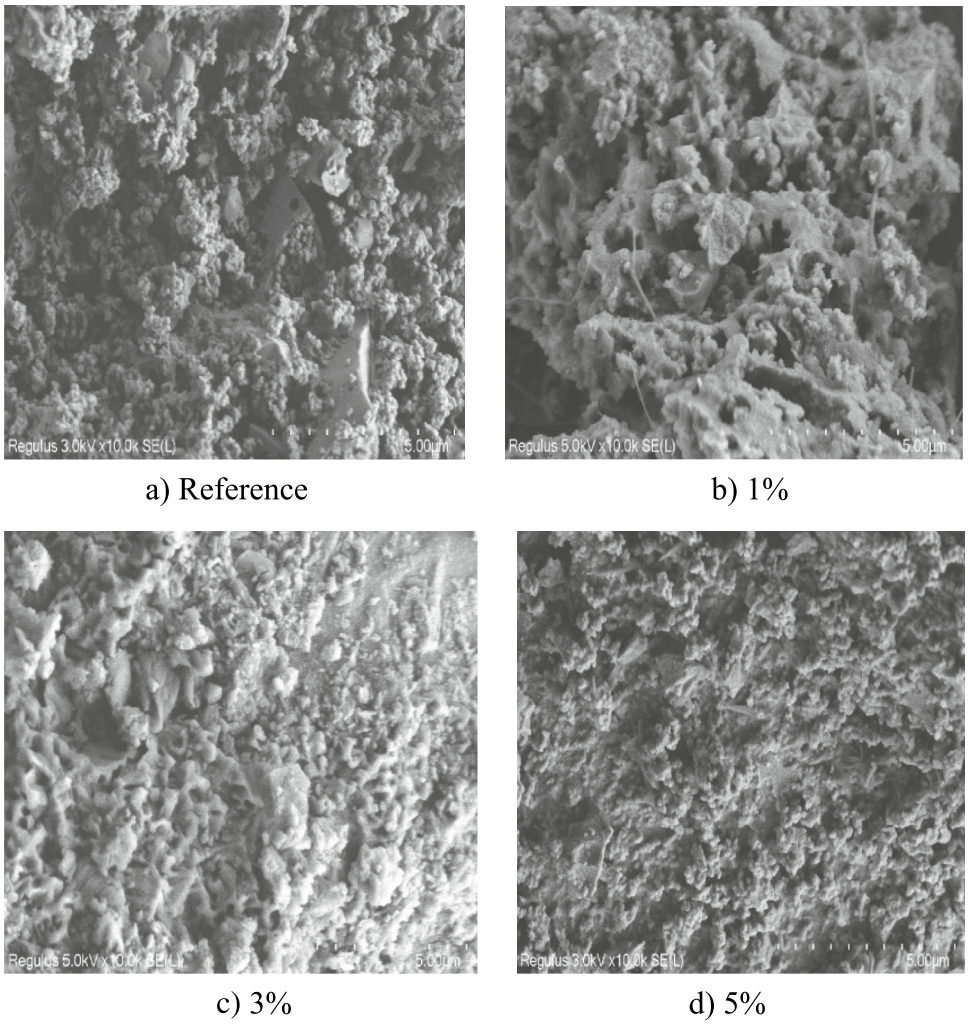


Fig.14 SEM images of the samples (×10,000 magnitude)

Table 4 ICP-MS analysis results

	Reference	1%	3%	5%
Al concentration average (ppb)	78.197	89.701	104.333	156.323
Al final quantity (ng)	4656	4194	4366	4828

NMR analysis

Figure 15 depicts the ^{27}Al MAS–NMR spectrum for geopolymers synthesized with aluminum-containing waste. The resonances of aluminum atoms are the same in all geopolymer samples.

In the ^{27}Al MAS-NMR spectrum for geopolymers, AlO6 (octahedral coordinates) signals are observed at 0–16 ppm, while AlO4 (tetrahedral coordinates) are seen at 55–80 ppm (Singh et al. 2005). The characteristic signals of geopolymers are Al(IV) or Al(4Si) signals in the reaction products that appeared around at 60 ppm, meaning aluminum atoms surrounded by four tetrahedral silicons (Criado et al. 2012; Peng et al. 2015; Dong et al. 2020). The characteristic Al(IV) signals observed for all alkali-activated aluminosilicates are assigned to aluminum in the mullite phase in fly ash (Peng et al. 2015).

The signals observed in the spectrum at 14 ppm and 65 ppm are attributed to hexa-coordinated and tetra-coordinated Al, respectively. The intensity of the signal of AlO4 (tetrahedral coordinates) slightly increased and shifted as the waste amount increased. The chemical shift of tetrahedral Al indicates its incorporation in the Si–O–Al bond of the geopolymeric gel phase (Xu et al. 2002).

Conclusion

This study demonstrates the effectiveness of an innovative electrocoagulation method for treating landfill leachate while promoting sustainable waste management by repurposing electrocoagulation sludge in geopolymer production. The

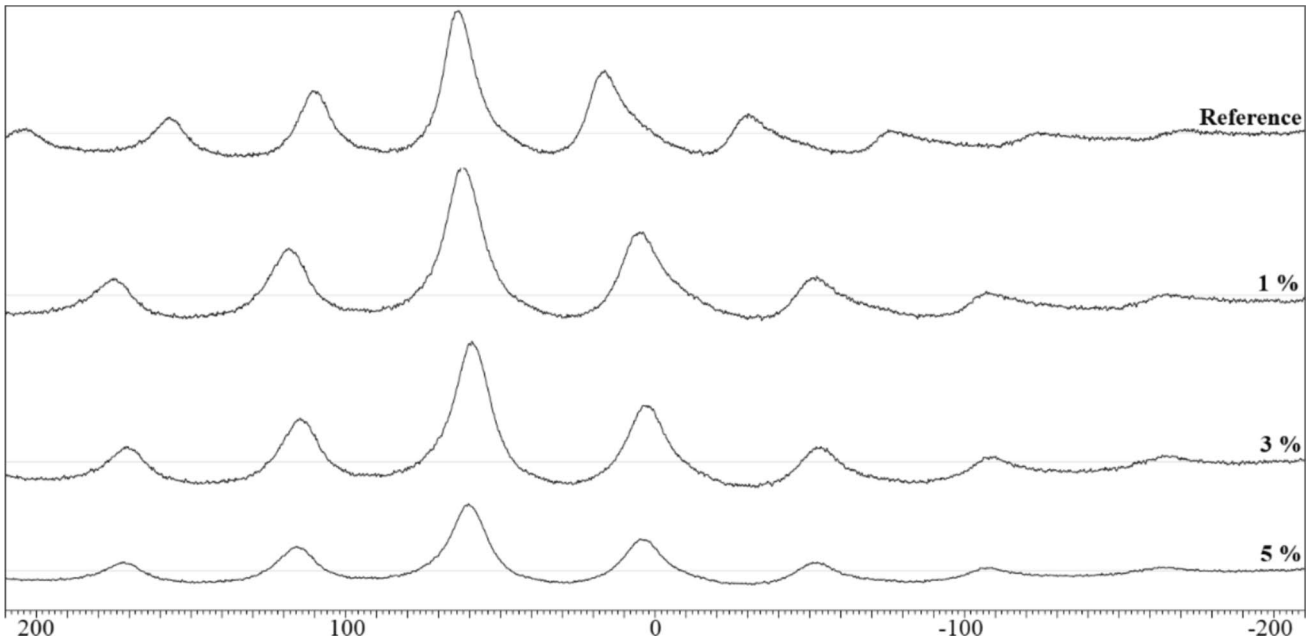


Fig. 15 NMR analysis charts for all samples

electrocoagulation process achieved significant pollutant removal efficiencies by optimizing key operational parameters, highlighting its potential as a viable and environmentally friendly treatment solution.

The experimental results revealed that the electrocoagulation process successfully removed 97% of COD, reducing its concentration from 9600 to 282 mg/L using pH 5, a current density of 40 mA/cm^2, a NaCl concentration of 0.1 M NaCl, and a stirring rate of 60 rpm, ensuring compliance with direct discharge regulations. Additionally, significant reductions in nutrient pollutants were observed, with phosphorus decreasing from 2.72 to below 0.5 mg/L and nitrogen levels dropping from 49 to 5 mg/L, meeting stringent environmental discharge standards.

Energy efficiency was also evaluated, revealing that increasing current density improved COD removal, and raised energy consumption. The study demonstrated that using 0.1 M NaCl as a supporting electrolyte reduced energy consumption from 59.4 to 30.7 kW h/m^3, showcasing the potential for cost-effective and sustainable electrocoagulation applications.

In addition to effective pollutant removal, the electrocoagulation process generated aluminum-rich sludge, which was successfully repurposed for geopolymer production. The sludge was incorporated into fly ash-based geopolymers at varying ratios (1%, 3%, and 5%) to assess its impact on material properties. XRF, XRD, FTIR, SEM, ICP-MS, and NMR analyses confirmed that the aluminum-containing sludge could be effectively integrated into the geopolymer matrix, contributing to structural stability while maintaining desired mechanical and chemical properties. The results indicated that mullite content increased with waste addition, improving the geopolymer's durability and sustainability. Additionally, the encapsulation of aluminum within the geopolymer structure minimized potential environmental concerns associated with its disposal, aligning with circular economy principles.

The findings of this study present a dual benefit: (1) a highly efficient and cost-effective method for landfill leachate treatment, reducing contamination risks to soil and water bodies, and (2) a sustainable approach to waste valorization, where electrocoagulation sludge is transformed into a valuable material for industrial applications. By integrating electrocoagulation with geopolymerization, this research provides a practical and scalable solution for wastewater treatment and sustainable material production. Future research can explore the long-term mechanical performance of geopolymer materials derived from electrocoagulation sludge and assess the economic feasibility of scaling up this integrated treatment approach.

Acknowledgements The authors are grateful to the Eskişehir Osmangazi University Scientific Research Projects Coordination Unit for funding this study under a research project (GR/FYL-2023-2623).

Author contributions Ayşegül Aşkin: Supervision, Project administration, Investigation, Data curation, Formal analysis, Methodology, Writing—original draft, Writing—review & editing, Conceptualization. Hanife Kübra Kirikbiçak: Investigation, Conceptualization, Data curation, Methodology, Writing—original draft. Evren Ariöz:

Conceptualization, Methodology, Writing—review & editing. Ümran Tezcan Ün: Conceptualization, Data curation, Methodology, Validation, Methodology, Writing—review & editing.

Funding Open access funding provided by the Scientific and Technological Research Council of Türkiye (TÜBİTAK). Eskişehir Osmangazi Üniversitesi, FYL-2023-2623, AYSEGÜL ASKIN

Data availability Data will be made available on request.

Declarations

Conflict of interest The authors declare that they have no known competing financial interests or personal relationships that could have appeared to influence the work reported in this paper.

Open Access This article is licensed under a Creative Commons Attribution 4.0 International License, which permits use, sharing, adaptation, distribution and reproduction in any medium or format, as long as you give appropriate credit to the original author(s) and the source, provide a link to the Creative Commons licence, and indicate if changes were made. The images or other third party material in this article are included in the article's Creative Commons licence, unless indicated otherwise in a credit line to the material. If material is not included in the article's Creative Commons licence and your intended use is not permitted by statutory regulation or exceeds the permitted use, you will need to obtain permission directly from the copyright holder. To view a copy of this licence, visit http://creativecommons.org/licenses/by/4.0/.

References

Abu-Nassar SO, Mokhtar Kamal NH, Halim H, Yusoff MS, Bashir MJK (2026) Performance and anode consumption of electrocoagulation and hybrid electrocoagulation–ultrasonic processes for optimized landfill leachate treatment. Jordan J Civ Eng 20:79–99. https://doi.org/10.14525/JJCE.v20i1.01

Akbar NA, Rahim MHA, Hakimi MN, Ismail BN, Mohd Zin NS, Hamid MAH, Said MS (2024) Removal of ammonia and colour from landfill leachate using integrated electrocoagulation-zeolite adsorption processes. Int J Integr Eng 16:454–465. https://doi.org/10.30880/ijie.2024.16.05.034

Anglada Á, Urtiaga A, Ortiz I, Mantzavinos D, Diamadopoulos E (2011) Boron-doped diamond anodic treatment of landfill leachate: evaluation of operating variables and formation of oxidation by-products. Water Res 45:828–838. https://doi.org/10.1016/j.watres.2010.09.017

American Society for Testing and Materials (1995) Standard test methods for chemical oxygen demand (dichromate oxygen demand) of water. D1252-95, ASTM Annual Book of Standards. American Society Testing & Materials, Philadelphia, Pa

Aouan B, Alehyen S, Fadil M, El Alouani M, Saufi H, El Herradi EH, El Makhoukhi F, Taibi M (2023a) Development and optimization of geopolymer adsorbent for water treatment: application of mixture design approach. J Environ Manage 338:117853. https://doi.org/10.1016/j.jenvman.2023.117853

Aouan B, Alehyen S, Fadil M, El Alouani M, Saufi H, Taibi M (2023b) Characteristics, microstructures, and optimization of the geopolymer paste based on three aluminosilicate materials using a mixture design methodology. Constr and Build Mater 384:131475. https://doi.org/10.1016/j.conbuildmat.2023.1314

Asaithambi P, Beyene D, Aziz AR, Alemayehu E (2018) Removal of pollutants with determination of power consumption from landfill leachate wastewater using an electrocoagulation process: optimization using response surface methodology (RSM). Appl Water Sci 8:69

Asaithambi P, Ezzat AO, Abd-Elkader OH, Al-Lohedan HA, Vigneshwaran S (2025) Investigation on operating parameters for efficient reduction of contaminants from wastewater utilizing a combined airlift, sono, and electrocoagulation techniques. Sci Rep 15:13716. https://doi.org/10.1038/s41598-025-13716-7

Atmaca E (2009) Treatment of landfill leachate by using electro-fenton method. J Hazard Mater 163:109–114. https://doi.org/10.1016/j.jhazmat.2008.06.067

Bayar S, Yilmaz AE, Zuhal Z, Boncukcuoglu R, Fil BA, Yilmaz MT (2015) The effect of initial ph on pistachio processing industrial wastewater pre-treatment by electrocoagulation method. In: Proceedings of the 2015 international conference on sustainable energy and environmental engineering. https://doi.org/10.2991/seee-15.2015.37

Bazrafshan E, Ownagh KA, Mahvi AH (2012) Application of electrocoagulation process using iron and aluminum electrodes for fluoride removal from aqueous environment. E-J Chem 9:2297–2308. https://doi.org/10.1155/2012/102629

Brett CMA, Brett AMO (1993) Electrochemistry: Principles, Methods, and Applications. Oxford University Press, Oxford

Castillo H, Collado H, Droguett T, Vesely M, Garrido P, Palma S (2022) State of the art of geopolymers: a review. E-Polymers 22:108–124. https://doi.org/10.1515/epoly-2022-0015

Chou WL, Wang CT, Chang SY (2009) Study of cod and turbidity removal from real oxide-cmp wastewater by iron electrocoagulation and the evaluation of specific energy consumption. J Hazard Mater 168:1200–1207. https://doi.org/10.1016/j.jhazmat.2009.02.163

Criado M, Fernández-Jiménez A, Sobrados I, Palomo A, Sanz J (2012) Effect of relative humidity on the reaction products of alkali-activated fly ash. J Eur Ceram Soc 32(11):2799–2807. https://doi.org/10.1016/j.jeurceramsoc.2011.11.036

Dong T, Xie S, Wang J, Chen Z, Liu Q (2020) Properties and characterization of a metakaolin phosphate acid–based geopolymer synthesized in a humid environment. J Aust Ceram Soc 56:175–184. https://doi.org/10.1007/s41779-019-00376-w

Faheem K, Khan SU, Washeem M, Khan SU (2021) Energy efficient removal of cod from landfill leachate wastewater using electrocoagulation: parametric optimization using RSM. Int J Environ Sci Technol 19:3625–3636. https://doi.org/10.1007/s13762-021-03277-3

Fernandes A, Spranger P, Fonseca AD, Pacheco MJ, Ciríaco L, Lopes A (2014) Effect of electrochemical treatments on the biodegradability of sanitary landfill leachates. Appl Catal B Environ 144:514–520. https://doi.org/10.1016/j.apcatb.2013.07.054

Fernandes A, Pacheco MJ, Ciríaco L, Lopes A (2015) Review on the electrochemical processes for the treatment of sanitary landfill leachates: present and future. Appl Catal B-Environ 176–177:183–200. https://doi.org/10.1016/j.apcatb.2015.03.052

Fernández-Jiménez A, Palomo A (2005) Mid-infrared spectroscopic studies of alkali-activated fly ash structure. Microporous Mesoporous Mater 86(1–3):207–214. https://doi.org/10.1016/j.micromeso.2005.05.05

Freire AL, Moura-Nickel CD, Scaratti G, De Rossi A, Araújo MH, De Noni Júnior A, Rodrigues AE, Castellón ER, de Fátima Peralta Muniz Moreira R (2020) Geopolymers produced with fly ash and rice husk ash applied to CO_2 capture. J Clean Prod 273:122917. https://doi.org/10.1016/j.jclepro.2020.122917

Galvão N, de Souza JB, Vidal CM (2020) Landfill leachate treatment by electrocoagulation: effects of current density and electrolysis time. J Environ Chem Eng 8:104368. https://doi.org/10.1016/j.jece.2020.104368

Gautam P, Kumar S, Vishwakarma S, Gautam A (2022) Synergistic optimization of electrocoagulation process parameters using

response surface methodology for treatment of hazardous waste landfill leachate. Chemosphere 290:133255. https://doi.org/10.1016/j.chemosphere.2021.133255

Guo Z, Zhang Y, Jia H, Guo J, Meng X, Wang J (2022) Electrochemical methods for landfill leachate treatment: a review on electrocoagulation and electrooxidation. Sci Total Environ 806:150529. https://doi.org/10.1016/j.scitotenv.2021.150529

Huang W, Wang H (2021) Geopolymer pervious concrete modified with granulated blast furnace slag: microscale characterization and mechanical strength. J Clean Prod 328:381–389. https://doi.org/10.1016/j.jclepro.2021.129469

Ilhan F, Kurt U, Apaydin O, Gonullu MT (2008) Treatment of leachate by electrocoagulation using aluminum and iron electrodes. J Hazard Mater 154(1-3):381–389. https://doi.org/10.1016/j.jhazmat.2007.10.035

Jamieson E, McLellan B, van Riessen A, Nikraz H (2015) Comparison of embodied energies of ordinary Portland cement with Bayer-derived geopolymer products. J Clean Prod 99:112–118. https://doi.org/10.1016/j.jclepro.2015.03.008

Jamil NH, Abdullah MMAB, Pa FC, Mohamad H, Ibrahim WMAW, Chaiprapa J (2020) Influences of SiO2, Al2O3, CaO, and MgO in phase transformation of sintered kaolin-ground granulated blast furnace slag geopolymer. J Mater Res Technol 9(6):14922–14932. https://doi.org/10.1016/j.jmrt.2020.10.045

Jegadeesan C, Somanathan A, Jeyakumar RB, Sharmila VG (2023) Combination of electrocoagulation with solar photo Fenton process for treatment of landfill leachate. Environ Technol 44:4441–4459. https://doi.org/10.1080/09593330.2022.2093654

Justen N, Borba FH, Mayer I, Seibert D, Inticher JJ, Ferreira Piazzi Fuhr AC, Carissimi E, Leichtweis J (2025) Advanced landfill leachate treatment: sequential electrocoagulation and electrooxidation system for efficient remediation. J Water Process Eng 74:107777. https://doi.org/10.1016/j.jwpe.2025.107777

Karagozoglu MB (2023) Treatment of landfill leachate via electrocoagulation and Electro-Fenton processes: a comparative study. Iran J Chem Chem Eng 42:2372–2391. https://doi.org/10.30492/ijcce.2023.1988851.5848

Kumar A, Yadav KD, Kumar S (2025) Optimisation of COD and TDS removal from hazardous waste landfill leachate by electrocoagulation process with varying electrode combinations using response surface methodology. Int J Environ Res 19:248. https://doi.org/10.1007/s41742-025-00916-2

Kumar S, Kumar R, Bandopadhyay A, Mehrotra SP (2007) Novel geopolymeric building materials through synergistic utilization of industrial waste. In: International conference alkali-activated materials: research, production and utilization, Prague

Kundu A, Kalamdhad AS (2026) Electrocoagulation-enhanced pretreatment for efficient operation of packed bed anaerobic filter treating leachate: kinetic and performance evaluation. Bioresour Technol 442:133770. https://doi.org/10.1016/j.biortech.2025.133770

Kundu A, Gupta N, Kalamdhad AS (2024) Optimization and kinetic analysis of electrocoagulation-assisted adsorption for treatment of young landfill leachate. J Environ Manage 366:121779. https://doi.org/10.1016/j.jenvman.2024.121779

Kuswah S, Mudgal M, Chouhan RK (2021) The process, characterization, and mechanical properties of fly ash-based solid form geopolymer via mechanical activation. S Afr J Chem Eng 38:104–114. https://doi.org/10.1016/j.sajce.2021.09.002

Lecomte I, Henrist C, Liégeois M, Maseri F, Rulmont A, Cloots R (2006) (Micro)-structural comparison between geopolymers, alkali-activated slag cement and Portland cement. J Eur Ceram Soc 26(16):3789–3797. https://doi.org/10.1016/j.jeurceramsoc.2005.12.021

Lessoued R, Baameur L, Tabchouche A (2021) Modeling and optimization of cod removal from leachate by electrocoagulation: application of central composite design. Environ Model Assess 26:423–432. https://doi.org/10.1007/s10666-021-09765-7

Li X, Song J, Guo J, Wang Z, Feng Q (2011) Landfill leachate treatment using electrocoagulation. Procedia Environ Sci 10:1159–1164. https://doi.org/10.1016/j.proenv.2011.09.185

Li R, Wang B, Owete O, Dertien J, Lin C, Ahmad H, Chen G (2017) Landfill leachate treatment by electrocoagulation and fiber filtration. Water Environ Res 89:2015–2020. https://doi.org/10.2175/106143017x15051465918976

Liu Y, Li Y, Jiang W, Chen M, Yang J, Li J (2017) Quantitative analysis on removal path of emulsified oil in the reactor of EC. Sep Purif Technol 178:288–297. https://doi.org/10.1016/j.seppur.2017.01.046

Liu J, Feng J, Wang Z, Lyu X, Liu C, Dai H, Bai Z (2023) Steel slag base geopolymer for efficient removal of Zn and Ni ions from aqueous solutions: preparation and characterization. Mater Lett 340:134173. https://doi.org/10.1016/j.matlet.2023.134173

Mansour D, El-Sofany WI, Abdella Faiza IA, Masood N, Khalaf Dhahi Alsukaibi A, Bellakhal N (2021) Doehlert experimental design for the optimization of electrocoagulation treatment of landfill leachate. Environ Pollut and Bioavailab 33:395–401. https://doi.org/10.1080/26395940.2021.1993752

Martínez-Huitle CA, Ferro S (2006) Electrochemical oxidation of organic pollutants for the wastewater treatment: direct and indirect processes. Chem Soc Rev 35:1324–1340. https://doi.org/10.1039/b517632h

Nath P, Sarker PK (2017) Flexural strength and elastic modulus of ambient-cured blended low-calcium fly ash geopolymer concrete. Constr Build Mater 130:22–31. https://doi.org/10.1016/j.conbuildmat.2016.11.03

Núñez J, Maril M, Pizarro-Castillo L, Lara C, Yeber M, Carrasco C (2024) Electrocoagulation of landfill leachate: transforming a hazardous residue into a source of irrigation water. J Environ Manage 370:122856. https://doi.org/10.1016/j.jenvman.2024.122856

Ogedey A, Oguz E (2024) Leachate treatment via electrocoagulation–coal–based powdered activated carbon process: efficiencies, mechanisms, kinetics, and costs. Water Environ Res 96:e11060. https://doi.org/10.1002/wer.11060

Peng Z, Vance K, Dakhane A, Marzke R, Neithalath N (2015) Microstructural and ^{29}Si MAS NMR spectroscopic evaluations of alkali cationic effects on fly ash activation. Cem Concr Compos 57:34–43. https://doi.org/10.1016/j.cemconcomp.2014.12.005

Pinedo-Hernández J, Marrugo-Negrete J, Pérez-Espitia M, Durango-Hernández J, Enamorado-Montes G, Navarro-Frómeta A (2024) A pilot-scale electrocoagulation-treatment wetland system for the treatment of landfill leachate. J Environ Manage 351:119681. https://doi.org/10.1016/j.jenvman.2023.119681

Pletcher D, Walsh FC (2012) Industrial Electrochemistry, 2nd edn. Springer Sci. and Bus, Media

Poggetto DS, Fortunato M, Cardinale AM, Leonelli C (2023) Thermal, chemical and mechanical characterization of recycled corundum powder in metakaolin-based geopolymer binder. Appl Clay Sci 237:106875. https://doi.org/10.1016/j.clay.2023.106875

Ramprasa C, Sona K, Afridhi M, Kumar R, Gopalakrishnan N (2019) Comparative study on the treatment of landfill leachate by coagulation and electrocoagulation processes. Nat Environ Pollut Technol 18(3):845–856

Singh SP, Trigg M, Burgar I, Bastow T (2005) Geopolymer formation processes at room temperature studied by ^{29}Si and ^{27}Al MAS-NMR. Mater Sci Eng A 396(1–2):392–402. https://doi.org/10.1016/j.msea.2005.02.002

Sudagar AJ, Andrejkovičová S, Rocha F, Patinha C, Velosa A, da Silva EF (2023) Compressive strength and heavy metal adsorption of cork residue, natural zeolite, and low-grade metakaolin-based geopolymers. Constr Build Mater 366:130125. https://doi.org/10.1016/j.conbuildmat.2022.130125

Temuujin J, Okada K, MacKenzie KJD (1999) Effect of mechano-chemical treatment on the crystallization behaviour of diphasic mullite gel. Ceram Int 25(1):85–90. https://doi.org/10.1016/S0272-8842(98)00005-4

Tezcan Un U, Oduncu E (2014) Electrocoagulation of landfill leachate with monopolar aluminum electrodes. J. of Clean Energy Technologies 2(1):15–17. https://doi.org/10.7763/JOCET.2014.V2.82

Tezcan Un U, Filik Iscen C, Oduncu E, Akcal Comoglu B, Ilhan S (2018) Treatment of landfill leachate using integrated continuous electrocoagulation and the anaerobic treatment technique. Environ Prog Sustain Energy 37(5):1668–1676. https://doi.org/10.1002/ep.12850

Water Pollution Control Regulations of Turkey (2004). https://www.mevzuat.gov.tr/mevzuat?MevzuatNo=7221&MevzuatTur=7&MevzuatTertip=5 (accessed 3 March 2024).

World Health Organization (2003) Guidelines for drinking-water quality, aluminium in drinking-water, background document for development of WHO guidelines for drinking-water quality. World Health Organ. https://iris.who.int/bitstream/handle/10665/75362/WHO_SDE_WSH_03.04_53_eng.pdf?se#:~:text=Dissolved%20aluminium%20concentrations%20in%20waters,water%20rich%20in%20organic%20matter (accessed 3 March 2024).

Xu H, Van Deventer JSJ (2002) Microstructural characterization of geopolymers synthesised from kaolinite/stilbite mixtures using XRD, MAS-NMR, SEM/EDX, TEM/EDX, and HREM. Cem Concr Res 32(11):1705–1716. https://doi.org/10.1016/S0008-8846(02)00859-1

Xu X, Bao S, Zhang Y, Luo Y, Qin L, Li S (2021) Role of particle fineness and reactive silicon-aluminum ratio in mechanical properties and microstructure of geopolymers. Constr Build Mater 313:125483. https://doi.org/10.1016/j.conbuildmat.2021.125483

Ye J, Zhang W, Shi D (2014) Effect of elevated temperature on the properties of geopolymer synthesized from calcined ore-dressing tailing of bauxite and ground-granulated blast furnace slag. Constr Build Mater 69:41–48. https://doi.org/10.1016/j.conbuildmat.2014.07.002

Yong-Sing N, Yun-Ming L, Cheng-Yong H, Abdullah MMAB, Rojviriya C, Khalid MS, Shee-Ween O, Wan-En O, Yong-Jie H (2023) Interaction of silica fume on flexural properties of 10 mm-thickness geopolymers based on fly ash and ladle furnace slag under the thermal conditions. J Build Eng 69:106331. https://doi.org/10.1016/j.jobe.2023.106331

Zahnoune R, Boudouch O, El Amri R, El Ghozlani M, Kamil N, Elkacmi R (2025) Optimized electrocoagulation and kinetic study for continuous treatment of fresh landfill leachate in an external-loop airlift reactor. Chem Eng Sci 317:122115. https://doi.org/10.1016/j.ces.2025.122115

Zhang J, Li S, Zhang C, Liu J, Zhang H, Xia Z, Zhang Y, Chen Y, Zhou M (2026) Insight into the Al-Fe dual-anode hybridperoxicoagulation-ozonation process for landfill leachate wastewater treatment: quantitative analysis of reaction pathways and synergistic mechanism. Water Res 288:124594. https://doi.org/10.1016/j.watres.2025.124594

Publisher's Note Springer Nature remains neutral with regard to jurisdictional claims in published maps and institutional affiliations.